International Journal for Multidisciplinary Research (IJFMR)
E-ISSN: 2582-2160 ● Website: www.ijfmr.com ● Email: editor@ijfmr.com

Mechanical and Thermal Characterization of Catalytic Converter Honeycombs Fabricated from Mfensi Clay-Based Composites

Mr. Asare Boakye Ansah[1], Prof. Nkrumah Isaac[2], Prof. Kwakye-Awuah Bright[3], Dr. Micheal Kweku Edem Donkor[4], Dr. Emmanuel Adu[5], Mr. Fred Joseph Komla Adzabe[6], Mr. Emmanuel Junior Budukumah[7], Mr. Obed Issakah[8]

Abstract

The study investigated the mechanical and thermal properties of catalytic honeycomb constructed from locally sourced Mfensi clay which was blended with silica, feldspar and Kaolin.

Feldspar, primarily made up of K-Feldspar and Gordonite, provides crucial mechanical strength and thermal stability, according to morphological and chemical characterization such as XRD studies. At high temperatures, Mfensi clay's substantial quartz component improves its refractoriness and structural stability. The presence of silicate and aluminate networks in the feldspar and Mfensi clay was also confirmed by the FTIR results; these networks have a significant impact on the material's thermal characteristics and ion exchange. They are quite important for the converter's effective catalytic activities. Distinct angular particles with smooth surface texture was identified by the SEM, this was confirmed by the EDX upon revealing the existence of oxygen, silicate and aluminum. The structure of Mfensi clay was elongated, columnar, and plate-like, with a somewhat uniform arrangement. The primary elements of silicon (Si), oxygen (O), and aluminum (Al) were validated by EDX analysis. Following a number of processing procedures, such as molding, controlled drying and firing at 1180 ℃, a fired shrinkage of 6.85% was obtained and this fired shrinkage could be a sign of good thermal integrity and dimensional stability, as well as temperature swings. The study's porosity of 33.1% obtained is within the ideal range of 25–45% for catalytic honeycombs. The compressive strength was 65.5 KN/mm^{-2} (6.55 MPa) and the thermal conductivity was 0.37 W/mK. These values are in line with those utilized for catalytic converter substrates based on mullite or alumina.

1.0. Introduction

The growing global challenge in air pollution has necessitated the need to look out for sustainable pathways through which emission from automobiles engines can be worked on, so that they come out clean into the environment (Patel et al., 2014), (Bergek et al., 2014). After combustion in the engine compartment , poisonous gases, such as carbon mono oxide, unburnt hydrocarbon and oxides of nitrogen are Produce and released eventually into the environment. Upon the release of these poisonous gases into the environment, they turn out to pose a great treat to the environment and its habitants (Patel et al., 2022). For instance, the carbon mono oxide released into the environment combine with the hemoglobin of the blood of humans when inhaled to form carboxyhemoglobin which is poisonous and could lead to the serious health issues and in worse cases causing death.

Pathways , needs to be developed to salvage the environment from such catastrophic pollutants. Catalytic converter have been known to be the most effective too that have been used over the years to control and covert these gases to less poisonous and environment friendly gases. The catalytic convertor has a honeycomb substrate that is responsible for the conversion of the pollutants. There are two main types, and they are the two-way and the three-way catalytic converters. The three way is mostly uses in automobile with petrol engines while the two way is aligned with the diesel engines. The TWC is responsible for two main reactions . They are responsible for oxidizing carbon monoxide into carbon dioxide , oxidizing the unburnt hydrocarbon into carbon dioxide and water and reducing the oxides of nitrogen into nitrogen gas (Gambarotta et al., 2019).

The substrate in the TWC is a ceramic product, which is manufactured from cordierite and mullite. These base materials are selected based on their excellent mechanical and thermal stability(Susan & Shukla, 2023).but their production and processing line makes the final product expensive. notwithstanding the fact that it is expensive, the TWC can also fail after it has been used for over one-hundred thousand kilometers (10000km) and when they fail, it becomes difficult for especially automobile users in developing countries like Ghana to purchase and replace. At the end the failed substrate is removed, and poisonous gasses are allowed directly into the environment without been converted. For the purposed of continuity, researchers are working around the clock to locate materials that are more accessible, preferably locally sourced, sustainable , cheap , excellent mechanical property and thermal stability to replace the existing ones (Twigg & Webster, 1998).

Natural aluminosilicate clay is in abundance and cheap as well. It can therefore be sourced as an alternative to the existing cordierite base honeycomb (Kovacev, 2022). Mfensi clay, a locally sourced clay from Ghana, was employed in this study as the base material for a catalytic substrate. The Mfensi clay was carefully combined with additives, such as silica to improve refractoriness, feldspar to promote liquid-phase sintering and densification, and kaolin to provide essential plasticity for honeycomb extrusion, the clay's potential was achieved. High porosity for effective gas diffusion, sufficient compressive strength to withstand mechanical shock, and outstanding thermal stability to withstand temperatures above $1000^{o}C$ are all functional requirements for the final composite (Ross et al., 2025).

By developing this new way to build catalytic honeycomb substrate from Mfensi clay, we are bridging the gap between local resources and high-tech engineering. This study's specific goals were to successfully produce a honeycomb substrate from the Mfensi clay composite using enhanced extrusion and high-temperature firing protocols; precisely measure mechanical and thermal properties, such as fired shrinkage, apparent porosity, compressive strength, and thermal conductivity; validate these parameters against established specifications for conventional catalytic substrates; and perform mineralogical and structural characterization of the material using XRD, FTIR, SEM, and EDX to confirm phase stability and microstructural integrity. Finally, this research aims to validate Mfensi clay as a resilient, sustainable, and cost-effective alternative to conventional catalytic converter substrates, promoting local resource use and supporting cleaner automotive emissions.

2.0. Methodology

The primary materials used in the development of the honeycomb structures included Mfensi clay, kaolin, feldspar, silica sand, zeolite, and water. In addition to these, several auxiliary materials and tools were employed during the preparation process, such as plaster of Paris (P.O.P), sieves of varying mesh sizes, and metal molds.

The clay obtained from Mfensi was dried, crushed and then sieved with a mesh to obtain very fine particle. The clay size was not uniform, because some particle sizes were finer than others.

The feldspar was extracted from its parent rock, then crushed, ground, and sieved to obtain the desired particle size. A mesh sieve was used to ensure uniformity, resulting in the required granulometry for the intended application The sand was also ground and sieved to obtain the required sizes. The method used was similar to the one used above. The kaolin was obtained in its raw state. In other to know that the primary materials (Mfensi clay and the feldspar) were viable for the preparation of a catalytic honeycomb , the following characterization were done: XRD, FTIR, SEM and EDX.

2.1. Preparation of the catalytic honeycomb

Table 1: The Various Compositions of Raw Materials Expressed In Percentages

Materials	*A*	*B*	*C*	*D*	*E*
Clay	42.1	36.8	31.8	26.3	21.1
Feldspar	5.3	5.3	5.3	5.3	5.3
Silica	10.5	10.5	10.5	10.5	10.5
Kaolin	42.1	43.4	53.3	57.9	63.2

Five different compositions of clay, feldspar, silica and kaolin as shown in Table 1. A typical catalytic converter honeycomb was produced through the process of forming , drying, firing at temperatures of 1050^oC and 1180^oC

The Mfensi clay, feldspar, silica and kaolin after they have been prepared were mixed until a uniform mixture was obtained. Some quantity was added to the prepared mixture until it attained the state at which casting could be done. The prepared clay mixture was transferred to a worktable where various molds had been set up for casting the honeycomb structures. Since the honeycomb differs in size from one automobile to the other different sample shapes were casted for the different samples used.

After forming, the honeycomb was dried, as much moisture as possible was removed from the honeycomb structure to prevent cracking or explosion in the kiln. The drying process involved the careful removal of moisture from the wet material to ensure uniform drying from the inside out. To enhance drying efficiency and uniformity, the honeycombs were periodically repositioned throughout the drying period.

The firing process proceeded the drying. An electric kiln was used for firing the honeycomb samples. The kiln operated on a 220 V power supply and could reach temperatures up to 1500^oC. For this study, the kiln was set to two specific firing temperatures of 1050 °C and 1180^oC depending on the sample batch. A honeycomb fabricated is as shown in figure 1

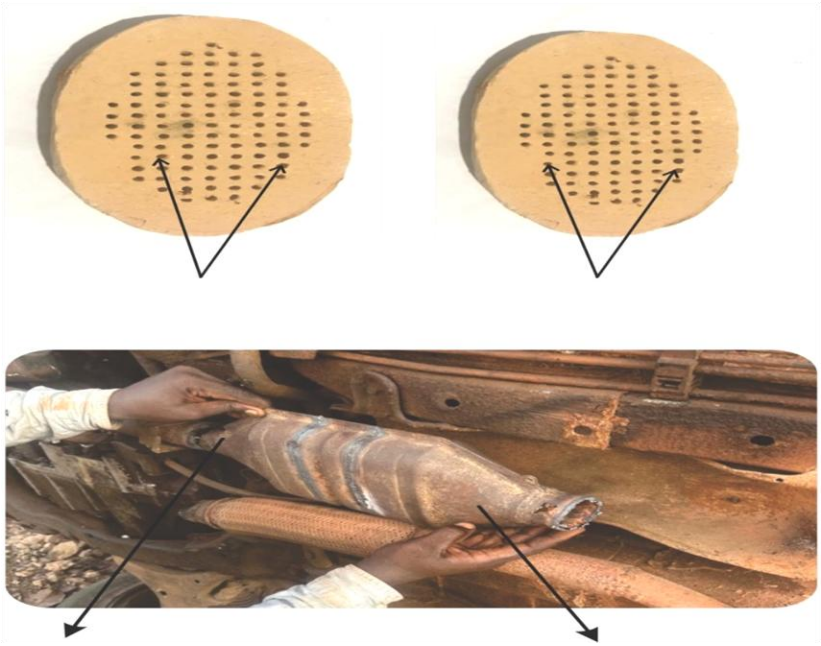

Figure 1: A picture of the fabricated honeycomb

2.2. Characterization of raw materials and fired honeycomb

Mfensi clay and feldspar were characterized using Xray diffraction. This was done by using a Bruker D2 Phaser instrument, operating at 30 kV and 10 mA with Cu Kα radiation for crystalline phase identification. Patterns were systematically collected across the 5° to 70° (2θ)range, utilizing a fine step size of 0.02° and a 2-second counting time per step to ensure high angular resolution. Fourier Transform Infrared Spectroscopy (FTIR) was conducted on a Bruker TENSOR 27 spectrometer in Attenuated Total Reflectance (ATR) mode to identify molecular functional groups. Spectra were recorded from 4500 to 500 cm^{-1} with an 8 cm^{-1} resolution and 128 scans, utilizing background subtraction for optimal signal-to-noise ratio. Finally, the surface morphology was studied using Scanning Electron Microscopy (SEM), here, a Nova NanoSEM 450 field-emission instrument at 20 KV was used and simultaneously the semi-quantitative elemental composition was determined through integrated Energy Dispersive X-ray Spectroscopy (EDX).

2.3. Physical, mechanical and thermal characterization of the honeycomb

Percentage dry and fired shrinkages were determined by first determining the green length, ambient dried length and the fired length. Prior to this, cubes were formed which were used in the determination of the shrinkages. After the green cube has been formed, a meter rule and a sharp object was used in drawing two diagonal line on top of the cube. Marks were made at the extreme vertices of the diagonals. The distance between these points was measured and recorded at three distinct stages of thermal processing. These included, points measured immediately after cube formation (Green length), points ,measured after sample has reached a constant dry stage(Dry length) and points measured after required fired treatment temperatures (Fired length).

The dry shrinkage and fired shrinkage were determined using equation 1 as shown below.

$$\%\ shrinkage = \frac{green\ length - dry\ or fired\ length}{green\ length} \times 100 \qquad (1)$$

The apparent porosity (PA) was determined through the Archimedes method (Moradi et al., 2014), calculating the ratio of the open pore volume to the bulk volume after 24-hourwater saturation and equation 2 was used in computing the values.

$$\%\ ApparentPorosity = \frac{Ws-Wa}{Ws-Ww} \times 100\ \%. \qquad (2)$$

W_a=Weight of dry sample in air

W_W = Weight of saturated sample in water

W_S = Weight of saturated sample in air

Compressive strength was assessed by determining the top and down areas and their average A was recorded . A load was applied to the measured surface area until structural failure, yielding the ultimate strength in MPa as described in equations below. The comprehensive strength was measured

$$Compressive\ strength = \frac{Crushing\ Load}{Area\ of\ sample\ on\ the\ plates} \qquad (3)$$

Where the crushing load is given by failure multiplied by machine factor (0.0258)

Finally, thermal conductivity (K) was measured using the Lee's Disc method under steady-state conditions, where the stabilized temperatures (T1, T2) allowed for the calculation of heat transfer through the clay composite (Mohapatra et al., 2014).

3.0. Results and Discussions

3.1. Physical and chemical composition of Mfensi clay composite that makes it possible to be used for the manufacture of a catalytic honeycomb substrate

The composite leverages Mfensi clay as the primary aluminosilicate source, the addition of silica and control feldspar acted as a critical fluxing agent to promote liquid-phase sintering (Smith & Jones, 2023). When the composite was fired to a temperature above 1000 ℃, the composite was now dominated by a crystalline phase mullite ($3Al_2O_3{\cdot}2SiO_2$) and residual quartz bound by an amorphous vitreous matrix (Lee & Chen, 2024, Adom & Mensah, 2022). This microstructure of the composite at this stage delivered the required high compressive strength and controlled, interconnected apparent porosity essential for exhaust gas flow and catalyst wash coat adhesion. The Mullite phase exhibited a low coefficient of thermal expansion, which then gave the composite the superior thermal shock resistance required of catalytic honeycomb substrates (Rodriguez & Patel, 2021). The morphological, physical, mechanical and thermal characterization of the Mfensi clay composite are discussed as shown below.

3.2. Morphological and Chemical Characterization of Raw Materials

3.2.1.X-Ray Diffractometry (XRD)

The mineralogical compositions identified from the XRD spectra are presented in Figure 2.

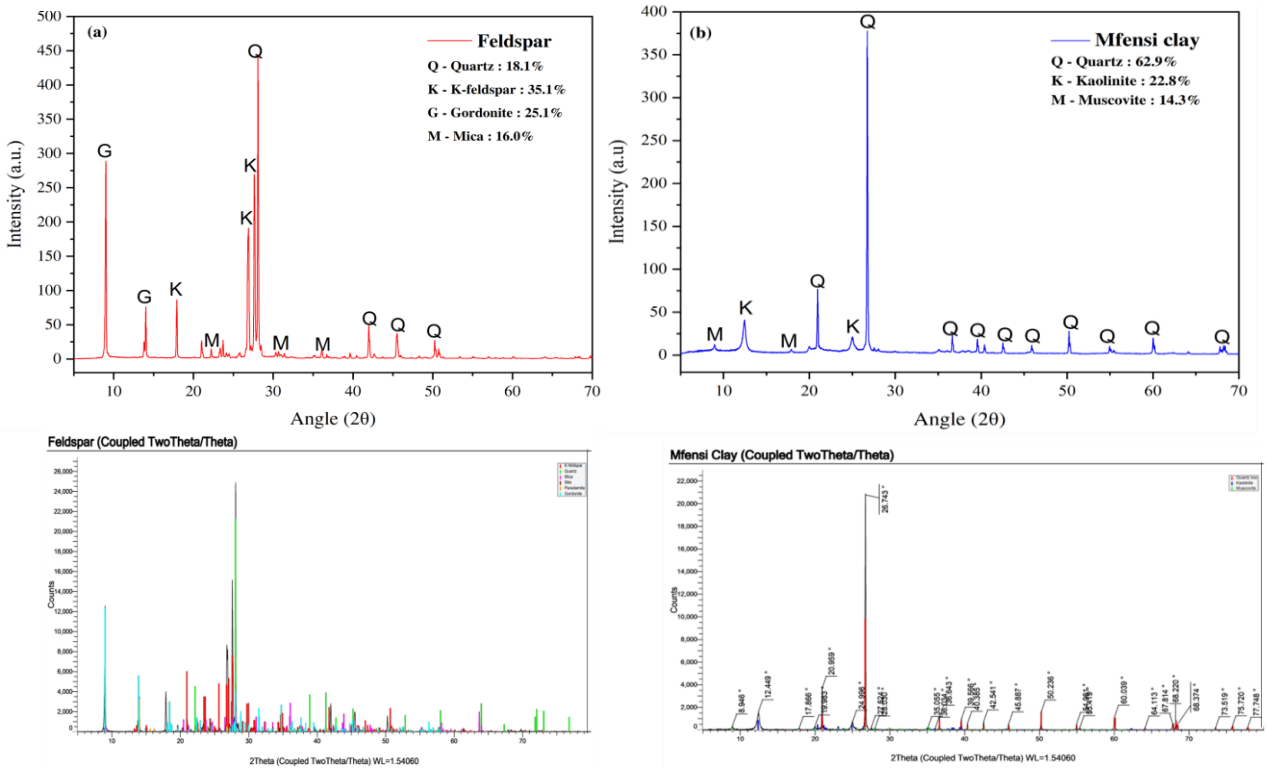

Figure 2. XRD spectra marked with major mineral components of (a) feldspar and (b) Mfensi clay.

The XRD analysis of the feldspar sample in Figure 2(a) revealed a composition dominated by K-feldspar (35.1%) and Gordonite (25.1%), with minor phases including mica and quartz. The composition of the feldspar sample in Figure 2(a) was found to be dominated by K-feldspar (35.1%) and Gordonite (25.1%), with mica and quartz being minor phases. Feldspar is composed of a family of tough minerals, including Gordonite and K-Feldspar, according to the testing (Kratz, 2022). These minerals serve as the crucial foundation for catalytic converters rather than being directly in charge of exhaust purification. They provide the rock-solid support that holds the catalyst such as platinum, palladium ,and rhodium together, ensuring these catalyst can perform their core functions even in the intense heat of an engine. Feldspar also influences the mechanical and thermal stability of the composite. a high content of K-Feldspar and Gordonite within the feldspar, prevents material degradation and mechanical failure in harsh thermal vibratory environment of a catalytic converter. This harsh thermal vibratory environment originates from continuous thermal expansion and contraction cycles (Upadhyay, 2025). This intrinsic properties of feldspar makes it a component for emission control device (Mrowczynski et al., 2023).

the XRD pattern in figure 2b for Mfensi clay identifies the following:62.9 % of quartz, 22.8 % of kaolinite, 11% of muscovite. This clearly makes quartz the predominant mineral. The sharp distinct peaks associated with quartz, confirms its crystalline nature. Quar4tzs being a hard crystalline with a Mohs hardness of 7 (Omotoyinbo et al., 2014) and taking into accounts its content in the Mfensi clay, would improve the properties of the clay.

furthermore, the high percentage of quartz in the Mfensi clay would enhance the clays chemical resistance and improve its refractoriness. As catalytic processes occurs at elevated temperatures, a high refractoriness of Mfensi clay would be an advantage (Lil et al., 2024). More importantly, mechanical stability, perfect gas flow and favorable catalytic reaction would be improved due to the presences of quartz (Hans-Joachim,1992).

3.2.2 Fourier-transform Infrared (FTIR) Spectroscopy

The presence of functional groups, which can greatly affect the materials' adsorption characteristics and general chemical behavior, was determined through FTIR analysis. Figure 3 (a) and (b) shows the FTIR spectra obtained.

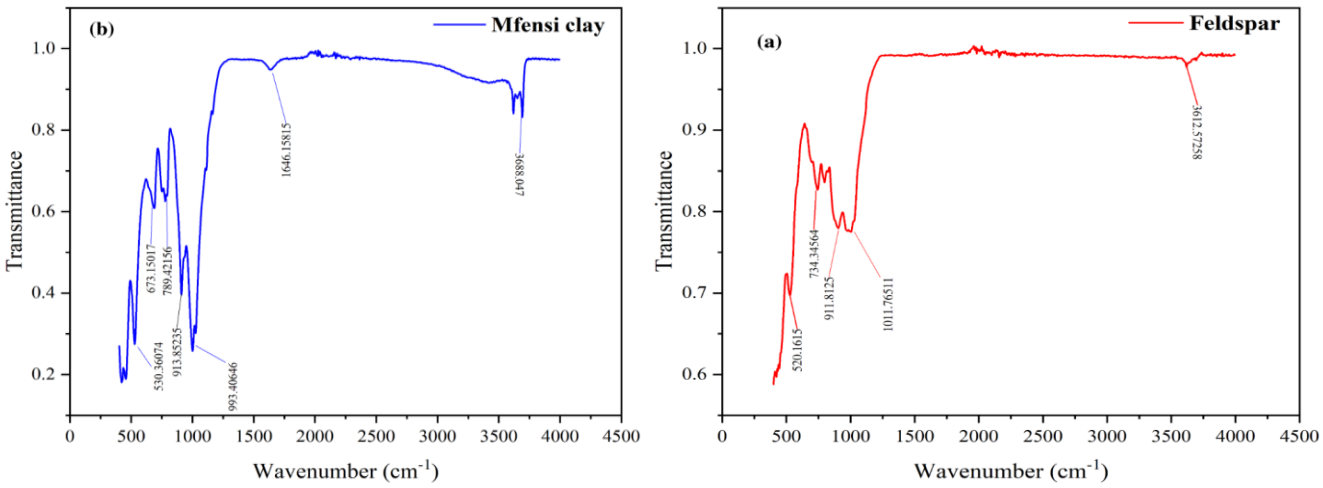

Figure 3: Fourier-transform Infrared (FTIR) spectra of the mineral components of (a) Feldspar and (b) Mfensi clay.

3.2.2.1. Feldspar FTIR Analysis

Si-O-Si stretching vibrations are characterized by a high, broad peak at 1011.76 cm^{-1} (Sagar & Singh, 2025), proving the existence of a strong silicate network that provides the structural backbone of quartz and feldspar and greatly adds to the material's mechanical strength. Al-O-Si vibrations are represented by weaker medium peaks at 734.34 cm^{-1} (Krishnamurthy et al., 2021), suggesting that aluminum has replaced silicon in the silicate network. The high aluminum content, which corresponds to Al-O-Al bonding, is further confirmed by the peak at 520.16 cm^{-1}. As shown in Figure 3(a), the feldspar spectra showed a shoulder medium band at 3612.57 cm^{-1}. Since pure feldspar normally lacks OH groups, this indicates the stretching of OH molecules, which is probably connected to muscovite or other hydroxyl impurities within the material (Wickramasuriya et al., 2021). These silicate and aluminate networks have a significant effect on the material's ion exchange and thermal characteristics, which are crucial for effective catalytic activity inside the converter

3.2.2.1.2 Mfensi Clay FTIR Analysis

The stretching vibrations of inner-surface hydroxyl groups, which are typical of kaolinite where aluminum primarily occupies octahedral locations, were represented by a spectral band at 3668.04cm^{-1} in the FTIR spectrum of Mfensi clay, as shown in Figure 3(b) (Mgbemere et al., 2020). Al-O bending, which is frequently seen in aluminosilicate minerals, is identified by a peak at 993.4 cm^{-1}, whereas the band at 913.85 cm^{-1} represents Al-O stretching that is typical of the kaolinite structure (Ncube et al., 2020). The presence of complex aluminosilicates typical of clays is reinforced by peaks at 673.15 cm^{-1} and 530.36 cm^{-1}, respectively, which are attributed to Si-O and Si-O-Fe stretches (Ncube et al., 2020, Nayak &Singh, 2007).

These structural components and functional groups are essential in determining the material's surface chemistry and gas interactions, which directly affect catalytic activity. Additionally, the O-H bending of

water molecules is shown as a peak at 1615 cm^{-1}. Kaolinite may have an innate ability to absorb pollutants due to its layered structure, which is beneficial for catalytic applications.

3.2.3. Scanning Electron Microscopy (SEM) and Energy Dispersive X-Ray (EDS) Analysis

The figures 4(a) and 4(b) show the results of the composition of elements and microstructural characteristics of the raw material feldspar

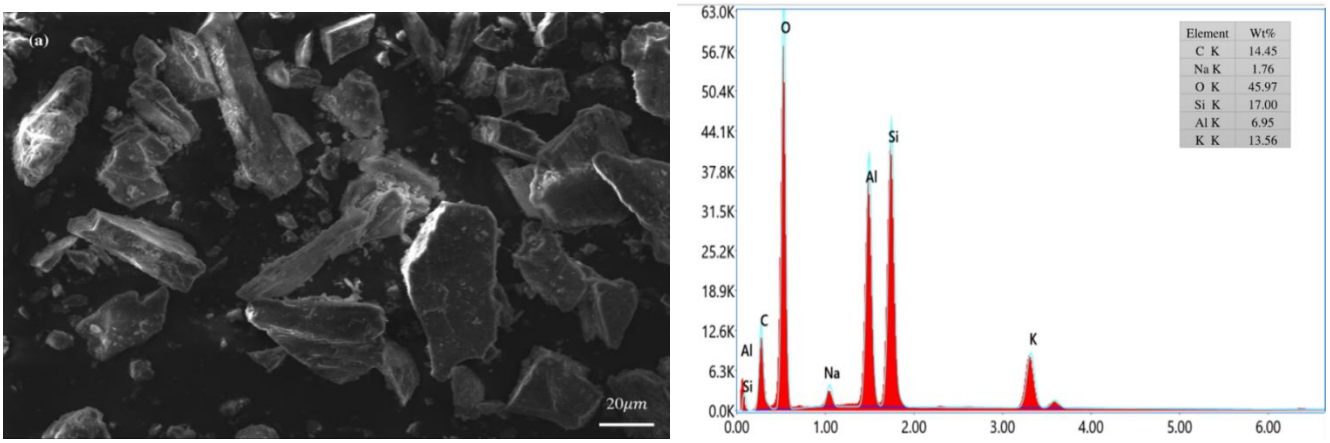

Figure 4a: Scanning electron microscopy (SEM) of feldspar.

Figure 4b: EDX spectra of Feldspar.

3.2.3.1. Feldspar Analysis

As displayed in Figure 4(a), a SEM study of feldspar showed discrete angular particles with smooth surface textures. Aluminum, silicate, and oxygen were confirmed to be present in the EDX spectra displayed in Figure 4(b). Also, certain impurities like potassium, carbon, and sodium were present. The angular shape of these particles improves shear strength and particle interlocking within the green body, which is advantageous for ceramic processing (Dong et al., 2021). From a catalytic standpoint, angular shapes' sharp edges and larger surface area can enhance mass transfer by creating more gas molecule collision points. This improves catalytic activity and boosts thermal stability by reducing sintering and increasing mechanical strength (Aldefae et al., 2020).

3.2.3.2. Scanning Electron Microscopy (SEM) and Energy Dispersive X-Ray (EDS) Analysis of Mfensi Clay

Figure 5 (a) and 5(b)shows the microstructural features and elemental composition of the raw material Mfensi clay

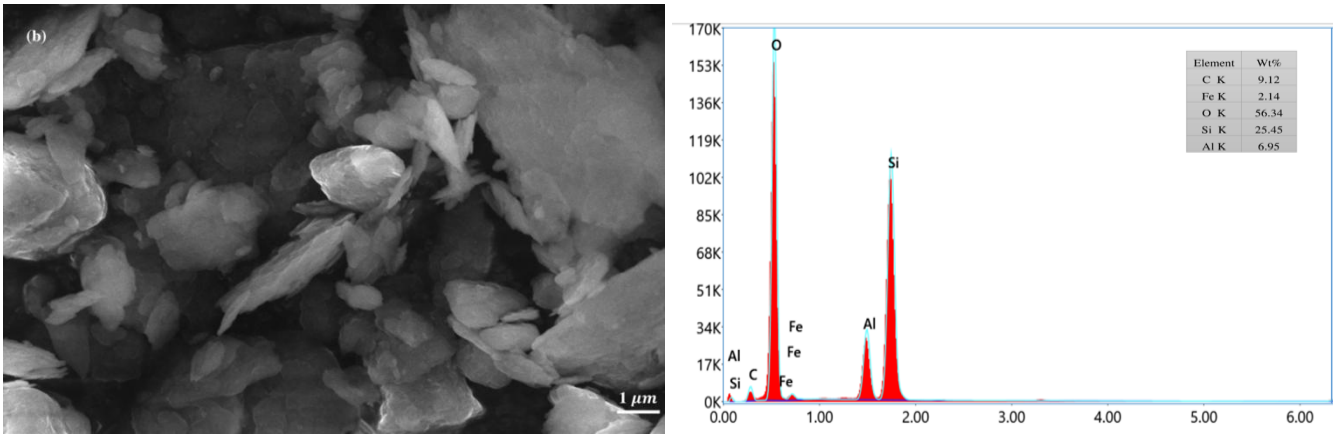

Figure 5(a): Scanning electron microscopy (SEM) of Mfensi clay.
Figure 5(b): EDX spectra of Mfensi clay.

3.2.3.2.1 Mfensi Clay Analysis

An extended columnar and plate-like morphology with a fairly regular arrangement was the main characteristic of the microstructure of the Mfensi clay, as shown in Figure 5(a) (Lawanwadeekul et al., 2023). The EDX analysis displayed in Figure 5(b) confirmed silicon (Si), oxygen (O), and aluminum (Al) as important elements, which was in line with earlier FTIR and XRD studies. Trace amounts of iron confirmed the presence of ferrous compounds (Gualtieri et al., 2013). The synergistic effect of this dual elongated columnar and platelike form is very beneficial for catalytic converter materials. In the end, by promoting optimal particle packing and porosity are both necessary for efficient gas flow and molecular diffusion, this combination shape increases overall catalytic efficiency and selectivity (Deng et al., 2023). In addition, through microstructural modification, this innate synergy offers the potential to adjust catalytic properties for specific uses

3.3. Physical characterization

3.3.1. Fired Shrinkage

Table 2: Average % Fired Shrinkage of Casted Samples at 1050 ℃ and 1180 ℃

Sample	*% Average Shrinkage at 1050* ℃	*% Average Shrinkage at 1180* ℃
A	6.29	8.57
B	5.27	8.86
C	5.71	6.85
D	5.43	7.42
E	6.0	10.0

Fired shrinkage is caused by progressive physiochemical densification, which is initiated by initial sintering below 1000 °C and further accelerated above this temperature by feldspar vitrification (Torres et al., 2025). Feldspar acts as a flux, filling pores with a glassy liquid phase that promotes the formation of mullite and interparticle bonding. This consistently resulted in significantly more shrinkage at 1180 °C (6.85 % to 10.0%) than at 1050 °C (5.27 % to 6.29 %). This discernible volume decrease at higher temperatures indicates the formation of a denser and more compact microstructure. Dimensional precision depends on maintaining small but enough shrinkage; Sample C's 6.85 % shrinkage at 1180 °C is within

acceptable bounds for ceramic substrates, indicating promising dimensional stability (Saleh and Hasan, 2025).

3.3.2. Apparent Porosity

The accessible surface area for catalyst wash coat deposition and gas flow dynamics are directly impacted by apparent porosity, a crucial indicator of the empty space within a ceramic material.

Table shows the average apparent porosity for casted samples at different firing temperatures

Table 3 : Average % Apparent Porosity of Casted Samples at 1050 ℃ and 1180 ℃

Sample	*% Average Apparent Porosity at 1050* ℃	*% Average Apparent Porosity at 1180* ℃
A	37.3	32.9
B	46.2	40.3
C	41.3	33.1
D	39.8	39.4
E	51.4	44.1

Apparent porosity consistently decreased at the higher firing temperature of 1180 ℃ and 1050 ℃. A direct result of improved vitrification and sintering that decreased the volume of linked pores in both sample types. The feldspar fluxing agent, which encourages the formation of a liquid phase at 1180 ℃ and results in superior densification and a subsequent decrease in water absorption capacity, is responsible for this temperature-dependent reduction. For catalytic honeycomb substrates, reaching the ideal porosity range of 25–45 % is essential.

3.4. Mechanical Characterization

3.4.1. Compressive Strength

A critical mechanical property of ceramic substrates is their compressive strength, which shows their ability to bear axial loads and survive breakage under operational pressures. Compressive strength testing were carried out in this study in compliance with ASTM C standards.

Table 4 shows the average compressive strength values for both cast and pressed samples, fired at 1050 °C and 1180 °C

Table 4 : Compressive Strength of Casted Samples ($KNmm^{-2}$ X 10^{-4})

Casted Sample	*Average Compressive Strength at 1050* ℃	*Average Compressive Strength at 1180* ℃
A	18.9	95.5
B	22.0	80.5
C	22.9	65.5
D	16.82	56.69
E	14.26	63.6

It is observed that the compressive strength of Mfensi clay casted was higher at higher temperature. For example, the compressive strength of casted sample c increased from 22.9×10^{-4} KN/mm at 1050^{o}C to 65.5×10−4 KN/mm^2 at 1180 (Abushama et al., 2023). At higher temperature, there is a decrease in the empty spaces in the material, and this may be the reason why a higher compressive strength is observed. Feldspar vitrification also creates a glassy liquid phase that helps in increasing the particle bond

encourages strong inter-particle bonding, which in this case increases the compressive strength [(Ben et al., 1998, Milisevic et al., 2019). The material's ability to withstand extreme mechanical stresses in automotive applications is confirmed by the high compressive strength values that arise, which satisfy the specifications for a lasting catalytic converter substrates.

3.5 Thermal Characterization

3.5.1. Thermal Conductivity

Thermal conductivity is an important characteristic of a catalytic honeycomb substrate. It is responsible for the regulation of heat inside the catalytic bed. It directly influences the reaction kinematics, reduces hot spot creation and ensures overall catalytic efficiency and thermal stability. The average thermal conductivity of casted samples is as shown in table 5 below.

Table 5 : Average Thermal Conductivity of Casted Samples at 1050 ℃ and 1180 ℃ (W/mK)

Casted Sample	***Average Thermal Conductivity at 1050 ^{O}C***	***Average Thermal Conductivity at 1180 ^{O}C***
A	0.44	0.32
B	0.41	0.38
C	0.38	0.37
D	0.45	0.41
E	0.62	0.56

An ideal thermal conductivity is essential for efficient heat management in catalytic applications, this is because, it controls temperature gradients over the catalyst bed and inhibits the development of localized hotspots that lead to catalyst deactivation (Folorunso et al., 2015). Overall catalytic stability and effective reaction kinetics depends on an even heat profile. A thermal conductivity value of 0.37W/mK by Mfensi clay composite aligns with standard catalytic honeycomb values (Onwusa et al., 2025),this makes the Mfensi clay composite a potential material for the use as catalytic converter substrate in in automobile

4.0. CONCLUSION

The manufacturing of catalytic converter honeycomb structures using Mfensi clay improved with feldspar, kaolin, and silica was successfully established in this work. Mineralogical and elemental compositions were confirmed by material characterization using X-ray diffraction (XRD), scanning electron microscopy (SEM), and energy dispersive X-ray spectroscopy (EDX), confirming the suitability of Mfensi clay for the intended use.

At a firing temperature of 1180 ℃ an apparent porosity of 33.1 % and a low fired shrinkage of 6.85 % were attained. The reasonable shrinkage attained, suggests a good dimensional stability over thermal changes, and the porosity value in a range of (25 %–45 %) falls within an ideal range for catalytic substrates. Furthermore, the material exhibited a high compressive strength of 6.55 MPa (65.5 KN/mm^2) and a thermal conductivity of 0.37 W/m^{3}K.These results show the material's capability for high-temperature and load-bearing conditions, as they are equivalent to those of traditional alumina or mullite-based catalytic converter substrates.

Importantly, different Mfensi clay compositions showed promising characteristics in all assessed metrics, suggesting a broad range of potential for this locally sourced resource. The reported relatively low thermal

conductivity may enhance heat distribution and control over catalytic reactions, even while the high compressive strength ensures durability and a longer service life. All things considered, this study demonstrates that Mfensi clay is a viable, economical, and sustainable alternative to the production of catalytic honeycomb. Future studies should focus on long-term durability under simulated operating conditions and investigating chemical interactions with various catalytic agents to fully realize its potential.

REFERENCES

1. Abushama, W. J., Tamimi, A. K., Tabsh, S. W., El-Emam, M. M., Ibrahim, A., & Mohammed Ali, T. K. (2023). Influence of optimum particle packing on the macro and micro properties of sustainable concrete. *Sustainability*, *15*(19), 14331.
2. Adom, P. Q., & Mensah, R. T. (2022). Microstructural Analysis and Vitrification in Local Ghanaian Clays Fired Above 1100∘C. *Materials Science Forum*, *106*(3), 88–95.
3. Aldefae, Asad H. Humaish, Abbas F. Essa, & Abbas S. Edan. (2020). "Fire Resistance of Selected Construction Materials." in *AIP Conference Proceedings*. Vol. 2213. American Institute of Physics Inc
4. Baehnisch, Hans-Joachim (1992). Catalytic reactor for compensating catalyst shrinkage in catalyst tubes - has catalyst supply hoppers fitted to catalyst tubes, with inernal vol. corresp. to catalyst.
5. Ben, M., Van, Vliet., Walter, J. & Weber (1998). Particle Surface Roughness Effects On The Interfacial Mass Transfer Dynamics of Microporous Adsorbents. Chemical Engineering Communications, 68(1):165-176. Doi: 10.1080/00986448808940404
6. Bergek, A., Berggren, C., & KITE Research Group. (2014). The impact of environmental policy instruments on innovation: A review of energy and automotive industry studies. *Ecological Economics*, *106*, 112-123.
7. Deng, B., Chen, Z., Sun, C., Zhang, S., Yu, W., et al. (2023). Key design and layout factors influencing performance of three-way catalytic converters: Experimental and semi decoupled numerical study under real-life driving conditions. *Journal of Cleaner Production*, *425*, 138993.
8. Dong, Z, Qiang S. & Weiqiang Z. (2021). "Physical and Mechanical Properties of Clay After Heating in Different Oxygen Levels and Cooling with Different Methods." doi: 10.21203/rs.3.rs-501548/v1.
9. Folorunso, D. O., Aribo, S., & Olaniran, O. (2015). Performance evaluation of insulating firebricks produced from hydro metallurgically purified Termite Hill clay reinforced with alumina. *American Journal of Engineering Research*, *4*(5), 1-7
10. Gambarotta, A., Papetti, V., & Dimopoulos Eggenschwiler, P. (2019). Analysis of the Effects of Catalytic Converter on Automotive Engines Performance Through Real-Time Simulation Models. *Frontiers in Mechanical Engineering*, *5*, 48.
11. Godbee, H.W and Ziglar, W.T (1966) Thermal Conductivity of MgO, Al_2O_3, ZrO2 powders to 850^0C. Pg 40 – 55
12. Gualtieri, M., Lassinantti, A. F., Gualtieri, S. G., Petra, R., Roberto, F. & Miriam, H. (2013). "Thermal Conductivity of Fired Clays: Effects of Mineralogical and Physical Properties of the Raw Materials." *Applied Clay Science* 49(3):269–75. doi: 10.1016/j.clay.2010.06.002
13. Kovacev, N. (2022). *Design and additive manufacturing of novel ceramic monolithic catalysts for low emission vehicles* (Doctoral dissertation, University of Birmingham)
14. Kratz, N. (2022). *10.4 Structural ceramics* (Vol. 231). Berlin, Germany: Walter de Gruyter GmbH & Co KG

15. Krishnamurthy, A., Razak, K. A., Halemani, B. S., Buradi, A., Afzal, A., & Saleel, C. A. (2021). Performance enhancement in tribological properties of lubricants by dispersing TiO2 nanoparticles. *Materials Today: Proceedings*, *47*, 6180-6184.
16. Lawanwadeekul, S., Anuwat, S., Nonthaphong, P., & Prinya, C. (2023). "Enhancement of Porosity and Strength of Clay Brick Fired at Reduced Temperature with the Aid of Corn Cob and Waste Glass." *Construction and Building Materials* 369:130547. doi: 10.1016/j.conbuildmat. 2023.130547 .
17. Lee, E. F., & Chen, G. H. (2024). High-Temperature Phase Evolution and Mullite Formation Kinetics in Kaolinitic Clay Systems. *Ceramics International*, *50*(1), 500–508.
18. Li, J., Huang, Y., Gao, M., Tie, J., & Wang, G. (2024) Shrinkage properties of porous materials during drying: a review. *Frontiers in Materials*, *11*, 13305999.
19. Mgbemere, H. E., Obidiegwu, E. O., & Ubong, A. U. (2020) The Effects of Sintering Temperature and Agro Wastes on the Properties of Insulation Bricks. *Nigerian Journal of Technological Development*, *17*(2), 113-119.
20. Milošević, M., Dabić, P., Kovač, S., Kaluđerović, L., & Logar, M.(2019) Mineralogical study of clays from Dobrodo, Serbia, for use in ceramics. *Clay Minerals*, *54*(4), 369-377.
21. Mohapatra, R. C., Mishra, A., & Choudhury, B. B. (2014). Experimental study on thermal conductivity of teak wood dust reinforced epoxy composite using Lee's apparatus method. *Int J Mech Eng Appl*, *2*, 98-103.
22. Moradi, A., Pramanik, S., Ataollahi, F., Kamarul, T., & Pingguan-Murphy, B. (2014). Archimedes revisited: computer assisted micro-volumetric modification of the liquid displacement method for porosity measurement of highly porous light materials. *Analytical Methods*, *6*(12), 4396-4401
23. Mrówczyński, D., Gajewski, T., & Garbowski, T. (2023). Sensitivity analysis of open-top cartons in terms of compressive strength capacity. *Materials*, *16*(1), 412.
24. Nayak, P. S., & Singh, B. K. (2007). Removal of phenol from aqueous solutions by sorption on low-cost clay. *Desalination*, *207*(1-3), 71-79
25. Ncube, S., Mlunguza, N. Y., Dube, S., Ramganesh, S., Ogola, H. J. O., Nindi, M. M., ... & Madikizela, L. M. (2020) Physicochemical characterization of the pelotherapeutic and balneotherapeutic clayey soils and natural spring water at Isinuka traditional healing spa in the Eastern Cape Province of South Africa. *Science of the Total Environment*, *717*, 137284.
26. Omotoyinbo, J. A., Oladele, I. O., & Shokoya, W. (2014). Effect of the degree of plastic deformation on the electrical resistance and thermal conductivity of Al-Mg-Si alloy. *Leonardo Electronic Journal of Practices and Technologies*, *13*(24), 37-50.
27. Onwusa, S. C., Umurhurhur, E. B., Afabor, A. M., Ighofimoni, M. I., Ekwemuka, J. U., & Uyeri, O. C. (2025). Influence of Fuel Types and Additives on the Efficiency of Catalytic Converter Materials in Automotive Applications. *UNIZIK Journal of Engineering and Applied Sciences*, *5*(2), 2421-2449.
28. Patel, A. K., Chaudhary, H. H., Patel, K. S., & Sen, D. J. (2014)Air pollutants all are chemical compounds hazardous to ecosystem. *World Journal of Pharmaceutical Sciences*, 729-744.
29. Patel, K. D., Subedar, D., & Patel, F. (2022). Design and development of automotive catalytic converter using non-nobel catalyst for the reduction of exhaust emission: A review. *Materials Today: Proceedings*, *57*, 2465-2472.
30. Rodriguez, I., & Patel, J. K. (2021). The Correlation Between Mullite Content and Thermal Shock Resistance in Extruded Ceramic Substrates. *Advanced Ceramic Materials*, *40*(4), 310–325.

31. Ross, M., Hoff, A. T., Hochstedler, W. M., Case, S., Finkenauer, L. R. (2025). Ceramic High Efficiency Particulate Air (HEPA) Filter Research and Development at Lawrence Livermore National Laboratory. *ACS Chemical Health & Safety*.
32. Sagar, P., & Singh, N.(2025) Characterization of Soil Nutrients by FTIR: Application to the Analysis of Micronutrients Changes in Soil affected by Food Crops.
33. Saleh, S., & Hasan, M. (2025). The effect of brick placement in the kiln during the burning process on clay brick properties. In *IOP Conference Series: Earth and Environmental Science* (Vol. 1477, No. 1, p. 012043). IOP Publishing.
34. Saxena, P., & Shukla, P. (2023) A review on recent developments and advances in environmental gas sensors to monitor toxic gas pollutants. *Environmental Progress & Sustainable Energy*, *42*(5), e14126.
35. Smith, A. B., & Jones, C. D. (2023). Role of Fluxing Agents in Promoting Low-Temperature Liquid-Phase Sintering of Ceramic Composites. *Journal of Materials Engineering*, *15*(2), 112–125.
36. Torres, P. M., Jahn, D., Ribeiro, N., Correia, T. R., Coelho, M., Carvalho, T. S., ... & Olhero, S. M. (2025). Enhancing bioactivity of calcium-phosphate cement-based 3D printed scaffolds with human platelet lysates: in vitro and in vivo validation. *Acta Biomaterialia*.
37. Twigg, M. V., & Webster, D. E. Metal and coated-metal catalysts. *Structured catalysts and reactors*, 59 (1998).
38. Upadhyay, R. K. (2025) Rocks and Their Formation. In *Geology and Mineral Resources* (pp. 351-421). Singapore: Springer Nature Singapore.
39. Wickramasuriya, A. I., Chandima Wickramasinghe Arachchige, R., & Kottegoda, I. R. (2021) Characterization and modification of clay for removal of drinking water hardness. *Mater. Sci. Res. India*, *18*, 318-331